Materials Letters 275 (2020) 128063

Contents lists available at ScienceDirect

Materials Letters

journal homepage: www.elsevier.com/locate/mlblue

EBSD study of superplastically strained Al-Mg-Li alloy

M. Myshlyaev [a,b], S. Mironov [c,*], G. Korznikova [d], T. Konkova [e], E. Korznikova [d], A. Aletdinov [d], G. Khalikova [d]

[a] Baikov Institute of Metallurgy and Material Science, Russian Academy of Science, 49 Lenin-av, Moscow 119991, Russia
[b] Institute of Solid State Physics, Russian Academy of Sciences, 2 Academic Osypian Str, Chernogolovka, Moscow Oblast 142432, Russia
[c] Belgorod National Research University, Pobeda 85, Belgorod 308015, Russia
[d] Institute for Metals Superplasticity Problems, Russian Academy of Science, 39 Khalturin Str, Ufa 450001, Russia
[e] University of Strathclyde, 75 Montrose Street, Glasgow G1 1XJ, United Kingdom

ARTICLE INFO

Article history:
Received 13 May 2020
Received in revised form 26 May 2020
Accepted 27 May 2020
Available online 4 June 2020

Keywords:
Superplasticity
Aluminium alloys
Microstructure
Electron backscatter diffraction

ABSTRACT

In this study, electron back scatter diffraction (EBSD) was employed to examine the microstructure evolved during superplastic deformation of advanced Al-Mg-Li alloy. In contrast to the widely-accepted conception of superplasticity, the microstructure was found to be characterized by elongated grains, a notable fraction of low-angle boundaries, and a distinct (though a very weak) crystallographic texture. All these observations suggested a significant activity of intragranular slip.

1. Introduction

Despite the phenomenon of superplasticity has been discovered ~100 years ago [1,2], it is still attracting a considerable research interest. This is due to a very unusual (or even exotic) nature of the involved microstructural mechanisms as well as the rapid development of superplastic forming in recent years. Current knowledge of the superplasticity is a result of extensive research over the last ~75 years. These works established the basic relationships between deformation conditions, the resulting microstructural processes and ductility, and thus enabled to develop a widely-accepted physical model of this phenomenon.

It is worth noting that our current understanding of the microstructural processes involved into the superplasticity is primarily based on observations from optical microscopy and transmission electron microscopy. However, a recent invention of electron backscatter diffraction (EBSD) provided new opportunities for investigation of this interesting phenomenon. This technique enables quantification of various microstructural details over very large scale thus opening a new dimension for microstructural analysis [3].

Indeed, the first EBSD studies of superplastically strained materials revealed a surprisingly high activity of intragranular deformation processes. Specifically, an extensive development of dynamic recrystallization has been found [e.g. 4–8]. So far, however, such studies are still limited.

The present work was undertaken to explore the microstructural behavior of advanced Al-Mg-Li alloy during superplastic deformation. This material belongs to a relatively new generation of aviation aluminum alloys with high specific strength and good weldability and having a good potential for application in aerospace industry.

2. Experimental

The material used in the present investigation was a commercial Al-5.5%Mg-2.2%Li-0.12%Zr (all wt.%) alloy supplied in a hot-rolled condition. To produce a fine-grained structure suitable for superplastic deformation, the received material was solutionized at 470 °C and then subjected to equal channel angular pressing (ECAP) at 370 °C. This produced a material condition with a mean grain size of ~3 μm, developed substructure, and a high fraction of dispersoids of Al_2LiMg and Al_3Li phases evenly distributed in grain interior.

The tensile specimen for superplastic test was machined along the axis of ECAPed billet and had a gauge section of 5 × 3 × 0.8 mm^3. The specimen was pulled to failure at 395 °C (≈0.72T_m, where T_m is the melting point) and the initial strain rate of 3×10^{-2} s^{-1} by using an Instron testing machine. The strain-rate-jump tests were employed to evaluate the strain-rate sensitivity parameter (m-value). To this end, crosshead velocity abruptly

* Corresponding author.
E-mail address: mironov@bsu.edu.ru (S. Mironov).

https://doi.org/10.1016/j.matlet.2020.128063
0167-577X/

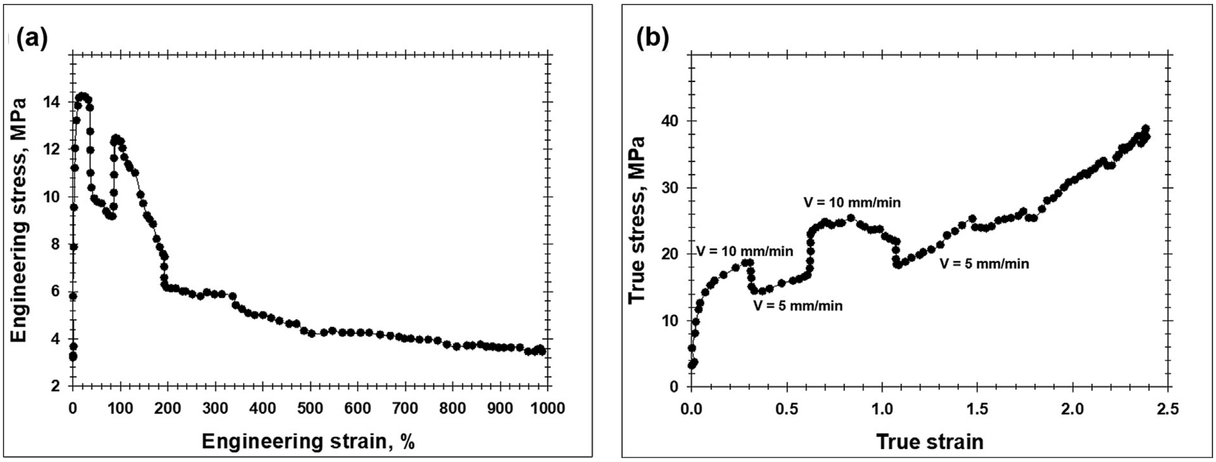

Fig. 1. Tensile behavior: engineering diagram (a) and true diagram (b). In (b), the variation of cross-head velocity.

changed from 10 to 5 mm/min and vice versa during the tensile tests. To enhance material ductility, the tensile tests were assisted by ultrasonic vibrations with frequency of 20 kHz and amplitude of 5 μm by using in-house acoustic system [9].

The final microstructure evolved in the gauge section of the failed specimen was studied by EBSD. The required surface finish was obtained by conventional metallographic technique followed by a long-term (24 h) vibratory polishing with colloidal silica. EBSD was conducted with a Hitachi S-4300SE field-emission-gun scanning electron microscope equipped with TSL OIM™ EBSD system and operating at accelerated voltage of 25 kV. To examine the microstructure at different length scales, several EBSD maps were acquired with a scan step size of 2 or 0.5 μm. To ensure reliability of EBSD data, all grains comprising two or fewer pixels were removed from the maps using the standard option of EBSD software. To eliminate the spurious boundaries caused by orientation noise, a lower limit boundary misorientation cut-off of 2° was employed. A 15° criterion was applied to differentiate low-angle boundaries (LABs) from high-angle boundaries (HABs).

3. Results and discussion

The flow curves recorded during the tensile test are shown in Fig. 1. From the engineering curve, the elongation-to-failure was measured to be ≈1,000% (Fig. 1a) and therefore the material, indeed, had experienced the superplastic deformation. The mean *m*-value was measured to be 0.4. It is also important to mention that the final stage of the true diagram was characterized by essential strain hardening (Fig. 1b) which presumably reflected an extensive intragranular slip activity.

Low-magnification EBSD map taken from the failed specimen is given in Fig. 2a. To investigate the microstructural distribution along the sample length, this map was divided into three microstructural regions, where Region 1 was located close to the sample shoulder, and Region 3 was close to the rupture location. To provide a closer inspection of the evolved microstructures, the higher-resolution EBSD maps obtained from these areas were shown in Fig. 2b to d. The appropriate microstructural data derived from the maps were summarized in Figs. 3 and 4.

From the above observations, it is seen that the microstructure distribution was very uniform thus suggesting a homogeneous character of material flow during superplastic deformation. In all cases, the final microstructure was dominated by the grains with the mean grain size of ~10 μm (Fig. 3a). This implied a significant coarsening of the original fine-grained structure during the superplastic deformation.

Of particular interest was the observation that the final grains were typically elongated along the tensile direction (Fig. 2b to d). Despite the mean grain shape aspect ratio[1] was measured to be 2, in some cases it achieved ~7 (Fig. 3b). Such grain morphology suggested an extensive slip occurring in grain interior.

Another significant issue was a notable fraction of LABs (12–15%) present in the superplastically-strained material. It is important, that the LABs were typically oriented perpendicular to the grain elongation (several examples are arrowed in Fig. 2b to d), as is often found in materials heavily deformed at high temperatures. It is possible, therefore, that the final microstructure dominated by low-aspect ratio grains originated from subdivision of elongated grains. This mechanism of microstructure evolution is well aligned with definition of continuous recrystallization. Despite the agreement with literature [4–8], the available microstructural data are not sufficient to definite conclusion to be drawn, and the assumption above require further thorough verification.

It is also important to emphasize that the superplastically strained material was characterized by a development of distinct crystallographic texture (Fig. 4). In all cases, the texture was dominated by the {*hkl*} ⟨1 0 0⟩ and {*hkl*} ⟨1 1 1⟩ fiber orientations which normally expected to form during axial tension of aluminum alloys [10]. Similar to the microstructure morphology described above, this texture observation also suggested a significant intragranular slip activity occurring during superplastic deformation.

Remarkably, the evolved texture was exceptionally weak with the peak intensity being below 2 times random (Fig. 4). In this context, it is worth noting that severe plastic deformation of a solutionized aluminum alloys (i.e., the grain-refinement processing similar to that used in the present work) may give rise to a decomposition of the supersaturated solid solution with the concomitant precipitation of a secondary phase along grain boundaries [11,12]. It is believed that such grain-boundary phase may exert a lubrication effect during subsequent superplastic deformation [13]. If so, it should partially relax the strain constraints between the neighboring grains and thus result in a poorly-developed texture, similar to that observed in the present study. Despite the prior microstructural observations revealed no signs of the grain-boundary phase in the studied material [14], the above mechanism is considered

[1] In this work, the grain shape aspect ratio was defined as the length of the major axis divided by the length of the minor axis of the ellipse fitting to the grain

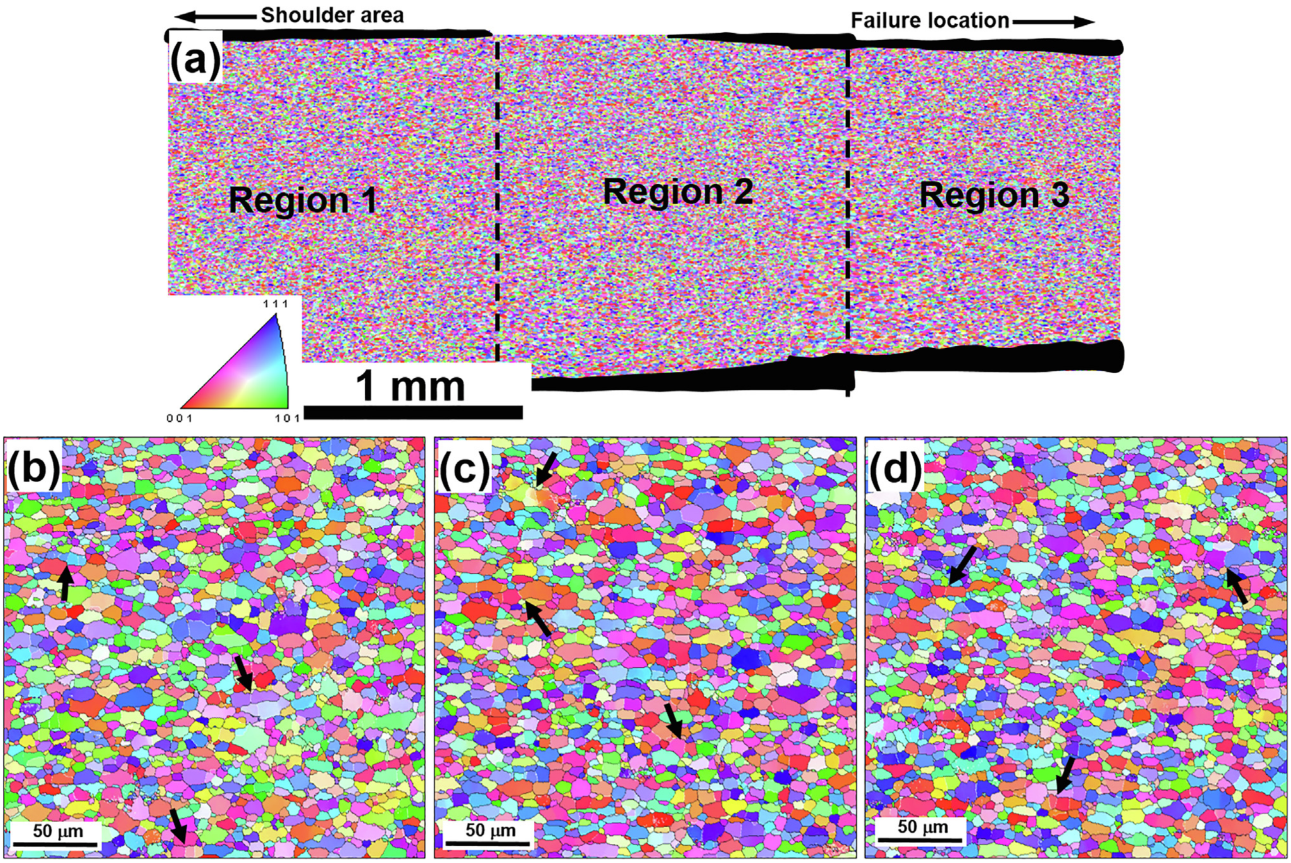

Fig. 2. Composite EBSD orientation map showing microstructure distribution in superplastically-deformed specimen (a) and higher resolution maps illustrating microstructure in Region 1 (b), Region 2 (c), and Region 3 (d). In all cases, individual grains in the maps are colored according to their crystallographic orientations relative to tensile direction; LABs and HABs are depicted as white and black lines, respectively. In (a), the grain boundaries are omitted for simplicity; in (b-d), examples of LABs are arrowed. Note: Tensile direction is horizontal.

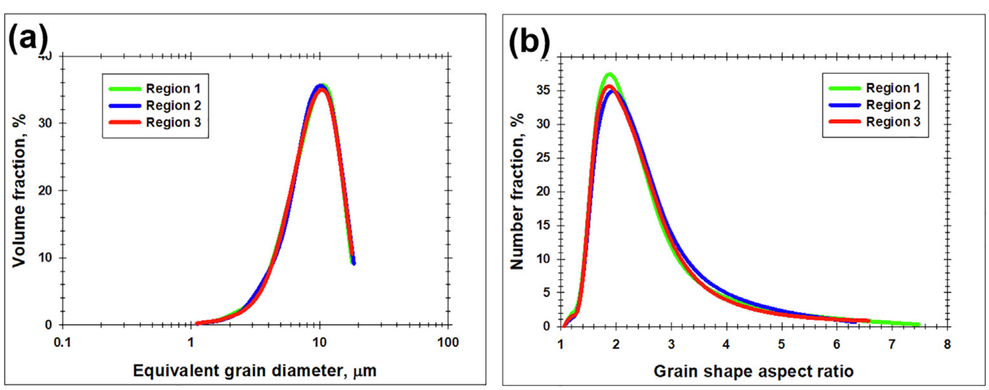

Fig. 3. Grain size distributions (a) and grain-shape-aspect-ratio distributions (b) measured in different locations of superplastically-deformed specimen.

reasonable in explaining of the textural data, and therefore this issue demands further study.

4. Conclusions

In this work, EBSD was applied to investigate a structural response of Al-Mg-Li alloy to superplastic deformation. The microstructure distribution in the gauge section of the superplastically-strained specimen was found to be fairly uniform thus indicating a very homogeneous character of material flow. In contrast to the widely accepted concept of superplastic deformation, the grains were found to be elongated along the tensile axis, contained a considerable fraction of LABs and were characterized by a crystallographic preference of orientations $\{hkl\}\langle 1\ 0\ 0\rangle$ and $\{hkl\}\langle 1\ 1\ 1\rangle$. All these observations suggested a considerable contribution of intragranular slip into global material flow.

From the analysis of microstructure morphology, it was surmised that the microstructural evolution was governed by a subdivision of elongated grains due to the development of LAB substructure, and, therefore, it fitted a definition of continuous recrystallization. On the other hand, it was recognized that this hypothesis was not supported enough by solid experimental data and thus additional verification is required.

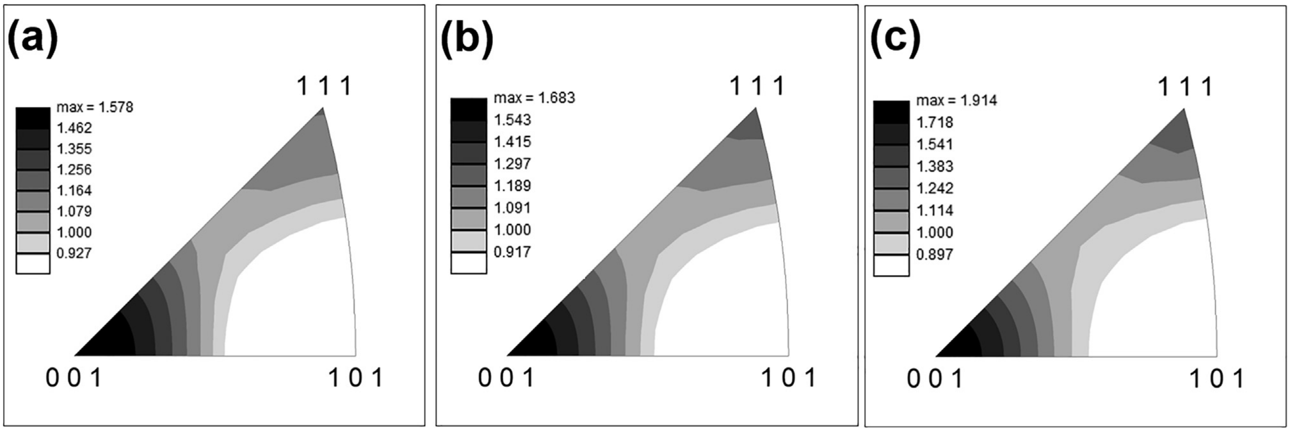

Fig. 4. Inverse-pole figures showing crystallographic orientation of superplastically-deformed material in Region 1 (a), Region 2 (b), and Region 3 (c).

CRediT authorship contribution statement

M. Myshlyaev: Conceptualization, Funding acquisition, Supervision, Project administration, Investigation, Validation, Writing - review & editing. **S. Mironov:** Conceptualization, Methodology, Investigation, Validation, Formal analysis, Visualization, Writing - original draft. **G. Korznikova:** Conceptualization, Supervision, Writing - review & editing. **T. Konkova:** Writing - review & editing. **E. Korznikova:** Writing - review & editing. **A. Aletdinov:** Formal analysis. **G. Khalikova:** Investigation.

Declaration of Competing Interest

The authors declare that they have no known competing financial interests or personal relationships that could have appeared to influence the work reported in this paper.

Acknowledgements

Financial support from the Russian Fund for Fundamental Research (project No.20-02-00331 A) is gratefully acknowledged. This work was also partially supported by the program of fundamental researches of IMSP RAS.

References

[1] D.G. Bengough, A study of properties of alloys at high temperatures, J. Inst. Met. 7 (1912) 123–174.

[2] C.E. Pearson, Viscous properties of extruded eutectic alloys of Pb-Sn, J. Inst. Met. 54 (1934) 111–123.

[3] B.L. Adams, S.I. Wright, K. Kunze, Orientation imaging: The emergence of a new microscopy, Met. Trans. A 24 (1993) 819–831, https://doi.org/10.1007/BF02656503.

[4] X.J. Zhu, M.J. Tan, W. Zhou, Enhanced superplasticity in commercially pure titanium alloy, Scripta Mater. 52 (2005) 651–655, https://doi.org/10.1016/j.scriptamat.2004.11.017.

[5] Z. Liu, P. Li, L. Xiong, T. Liu, L. He, High-temperature tensile deformation behavior and microstructure evolution in Ti55 titanium alloy, Mater. Sci. Eng. A 680 (2017) 259–269, https://doi.org/10.1016/j.msea.2016.10.095.

[6] F.C. Liu, P. Xue, Z.Y. Ma, Microstructural evolution in recrystallized and unrecrystallized Al-Mg-Sc alloys during superplastic deformation, Mater. Sci. Eng. A 547 (2012) 55–63, https://doi.org/10.1016/j.msea.2012.03.076.

[7] S.W. Xu, M.Y. Zhenh, S. Kamado, K. Wu, The microstructural evolution and superplastic behavior at low temperatures of Mg-5.00Zn-0.92Y-0.16Zr (wt.%) alloys after hot extrusion and ECAP process, Mater. Sci. Eng. A 549 (2012) 60–68, https://doi.org/10.1069/j.msea.2012.03.116.

[8] A.V. Mikhaylovskaya, O.A. Yakovtseva, I.S. Golovin, A.V. Pozdniakov, V.K. Portnoy, Superplastic deformation mechanisms in fine-grained Al-Mg based alloys, Mater. Sci. Eng. A 627 (2015) 31–41, https://doi.org/10.1016/j.msea.2014.12.099.

[9] M.M. Myshlyaev, V.V. Speizman, V.V. Klubovich, M.M. Kulak, G. Lyu, Change in characteristics of superplastic deformation of the aluminum-lithium alloy under the effect of ultrasonic vibrations, Phys. Sol. State. 57 (2015) 2039-2044; https://doi.org/10.1134/S1063783415100236

[10] J. Savoie, Y. Zhou, J.J. Jonas, S.R. Macewen, Textures induced by tension and deep drawing in aluminum sheets, Acta Materialia 44 (1996) 587–605, https://doi.org/10.1016/1359-6454(95)00214-6.

[11] A.A. Mazilkin, B.B. Straumal, M.V. Borodachenkova, R.Z. Valiev, O.A. Kogtenkova, B. Baretzky, Gradual softening of Al-Zn alloys during high-pressure torsion, Mater. Letter., 84 (2012) 63-65; https://doi.org/10.1016/j.matlet.2012.06.026

[12] N.Q. Chinh, R.Z. Valiev, X. Sauvage, G.Varga, K. Havancsak, M. Kawasaki, B.B. Straumal and T.G. Langdon, Grain boundary phenomena in an ultrafine-grained Al-Zn alloy with improved mechanical behavior for micro-devices, Adv. Eng. Mater. 16 (2014) 1000-1009; https://doi.org/10.1002/adem.201300450

[13] B.B. Straumal, A.O. Rodin, A.E. Shotanov, A.B. Straumal, O.A. Kogtenkova, B. Baretzky, Pseudopartial grain boundary wetting: key to the thin intergranular layers, Def. Diff. Forum 333 (2013) 175–192, https://doi.org/10.4028/wwwscientific.net/DDF.333.175.

[14] A.A. Mazilkin, M.M. Kamalov, M.M. Myshlyaev, Structure and phase composition of an Al-Mg-Li-Zr alloy under high-rate superplasticity conditions, Phys. Solid State 46 (2004) 1456–1461, https://doi.org/10.1134/1.1788778.